

Infrared Lattice Vibrations and Dielectric Dispersion in Single-Crystal Cr_2O_3 †

D. R. RENNEKE* AND D. W. LYNCH

Institute for Atomic Research and Department of Physics, Iowa State University, Ames, Iowa

(Received 19 November 1964)

Reflectivity measurements on single-crystal Cr_2O_3 have been made at room temperature in the wavelength range 1 to 45 μ . A classical oscillator analysis of the data has determined the frequencies, strengths and line-widths of the optical-lattice vibration modes with dipole moment vibrating parallel and perpendicular to the c axis. The modes vibrating parallel to the c axis occur at 538 and 613 cm^{-1} . Those vibrating perpendicular to the c axis occur at 417, 444, 532, and 613 cm^{-1} . Forbidden modes, believed to be caused by surface shear strains, have been observed. Vibration frequencies of long-wavelength longitudinal modes corresponding to the transverse vibration frequencies quoted above were calculated from the zeros of the real part of the dielectric constant. These values offer excellent experimental verification of the generalized Lyddane-Sachs-Teller equation derived by Kurosawa and by Cochran and Cowley. Comparison of the transverse-optic-mode frequencies of Cr_2O_3 with those of $\alpha\text{-Al}_2\text{O}_3$ shows a considerable increase in force constants for the former, probably due to increased covalent bonding in Cr_2O_3 .

INTRODUCTION

THE purpose of this investigation was to characterize the infrared optical lattice modes of Cr_2O_3 from a classical oscillator analysis of its reflectivity data. This analysis in turn determined the static and high-frequency dielectric constants (ϵ_0 and ϵ_∞) for the two cases of dipole moment vibrating parallel and perpendicular to the c axis of the crystal. The effect of magnetic ordering on the reflectivity was investigated by performing all measurements at room temperature and at 313°K (above the Néel temperature of 307°K)¹ but no significant difference was ascertained.

Much work has been done on the optical properties of $\alpha\text{-Al}_2\text{O}_3$ (corundum, to be referred to just as Al_2O_3 in the following), in particular by Barker.² Since Cr_2O_3 and Al_2O_3 have nearly identical crystal structure, one would expect comparable results. The symmetry of these lattices predicts³ two infrared active modes when the electric vector is parallel to the c axis of the crystal ($E\parallel C$) and four active modes $E\perp C$. The experiments with Al_2O_3 and this work both detect these modes along with several forbidden modes.

The most elementary approach to the optical properties of ionic crystals is to consider a single classical oscillator and solve the equations of motion to obtain the Lorentz formulas for the real and imaginary parts of the dielectric constant. For complex crystals a series of classical oscillators are needed to explain the observed optical dispersion. Summing over all oscillators, the expressions for the real and imaginary dielectric con-

stants⁴ are

$$\epsilon_1(\nu) = \epsilon_\infty + \sum_j \frac{4\pi\rho_j\nu_j^2(\nu_j^2 - \nu^2)}{(\nu_j^2 - \nu^2)^2 + \gamma_j^2\nu^2}, \quad (1)$$

$$\epsilon_2(\nu) = \sum_j \frac{4\pi\rho_j\nu_j^2\gamma_j\nu}{(\nu_j^2 - \nu^2)^2 + \gamma_j^2\nu^2}, \quad (2)$$

where ν_j , $4\pi\rho_j$, and γ_j (the dispersion parameters) are the frequency, strength, and linewidth, respectively, of the j th oscillator and ϵ_∞ is the high-frequency dielectric constant. The static dielectric constant ϵ_0 is then

$$\epsilon_0 = \epsilon_\infty + \sum_j 4\pi\rho_j. \quad (3)$$

The reflectivity at normal incidence is

$$R = \frac{(n-1)^2 + k^2}{(n+1)^2 + k^2}, \quad (4)$$

where n and k are the real and imaginary parts of the complex refractive index N ,

$$N = n - ik = (\epsilon_1 - i\epsilon_2)^{1/2}. \quad (5)$$

Equations (1), (2), (4), and (5) permit curves of reflectivity versus ν to be calculated with various sets of dispersion parameters.

Cr_2O_3 has a trigonal structure similar to corundum and is antiferromagnetic.¹ A comparison of the interatomic spacings in Al_2O_3 ,⁵ and in Cr_2O_3 ,⁶ reveals that most interatomic spacings are larger in Cr_2O_3 .

EXPERIMENTAL PROCEDURE

The single crystal of Cr_2O_3 used in this experiment was obtained from Semi-Elements Inc., Saxonburg, Pennsylvania. Its approximate dimensions were $\frac{1}{4}$ -in.

† Contribution No. 1606. Work was performed in the Ames Laboratory of the U. S. Atomic Energy Commission.

* Present address: Department of Physics, University of Kansas, Lawrence, Kansas.

¹ T. R. McGuire, E. J. Scott, and F. H. Graunis, *Phys. Rev.* **102**, 1000 (1956).

² A. S. Barker, *Phys. Rev.* **132**, 1474 (1963).

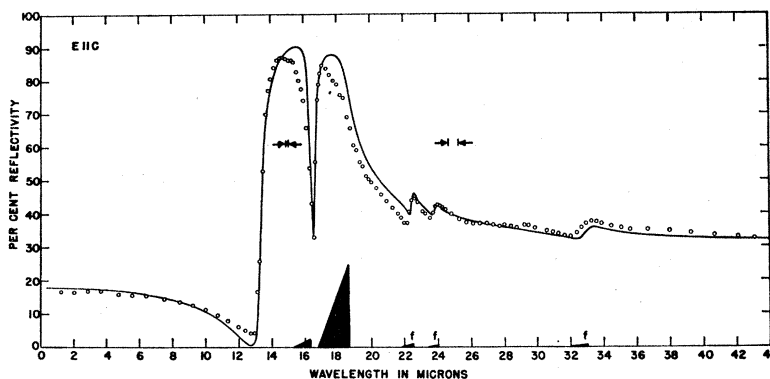
³ S. Bhagavantam and T. Venkatarayudu, *Proc. Indian Acad. Sci.* **9A**, 224 (1939).

⁴ F. Seitz, *Modern Theory of Solids* (McGraw-Hill Book Company, Inc., New York, 1940), Chap. 17.

⁵ S. Geschwind and J. P. Remeika, *Phys. Rev.* **122**, 757 (1961), and references therein.

⁶ R. E. Newnham and Y. M. deHaan, *Z. Krist.* **117**, 235 (1962).

FIG. 1. Reflectivity of Cr_2O_3 for $E\parallel C$. The solid line is the best 5-mode classical oscillator fit. In this and the following figure, each shaded right triangle represents an oscillator. The right edge of each triangle is located at the transverse frequency of the oscillator. The height of each triangle is proportional to the oscillator strength where $4\pi\rho=1$ is given an ordinate of 5% reflectivity. The width of the triangle base is proportional to the oscillator width where $\gamma=1$ is given a distance of $0.2\ \mu$ on the wavelength scale. The arrows indicate the spectral band width of the monochromator.



diam \times 1 in. long. The crystal was cut on a diamond saw with the c axis in the plane of the cut. This plane was polished with Grade 3 medium diamond compound ($0\text{--}5\ \mu$ grain size) in oil on Microcloth. Finally, a Laue x-ray reflection pattern of the polished face was obtained to determine the orientation of the c axis in the plane. The c axis was within 4° of the plane of the face. Unfortunately only one single crystal of appropriate size was available to us.

The apparatus consisted of a Perkin-Elmer model 112 double-pass infrared spectrometer with attached accessory table. The light source was a globar whose light intensity was maintained at a constant level to within $\pm 0.1\%$ by a voltage regulator. A rotatable transmission polarizer was inserted between the source box and the monochromator. For wavelengths up to about $20\ \mu$, a Perkin-Elmer 6-plate AgCl polarizer was used. At longer wavelengths a 15-plate polyethylene polarizer⁷ was used. The crystal was in the monochromatic polarized beam from the monochromator. LiF , NaCl , KBr , and CsI prisms were used. At longer wavelengths LiF or CaF_2 reststrahlen plates were used in place of an aluminum mirror just preceding the sample to reduce shorter wavelength radiation.

The reflectivity was measured by comparing the reflected intensity from the sample with that from a front-surface aluminized mirror which was coated with

SiO . Since the crystal was slightly smaller than the image of the exit slit, masks were used over the crystal and standard. All measurements were made using plane-polarized light incident on the crystal either parallel to the c axis of the crystal ($E\parallel C$) or perpendicular ($E\perp C$). The angle of polarization was changed by rotating the polarizer rather than the sample.

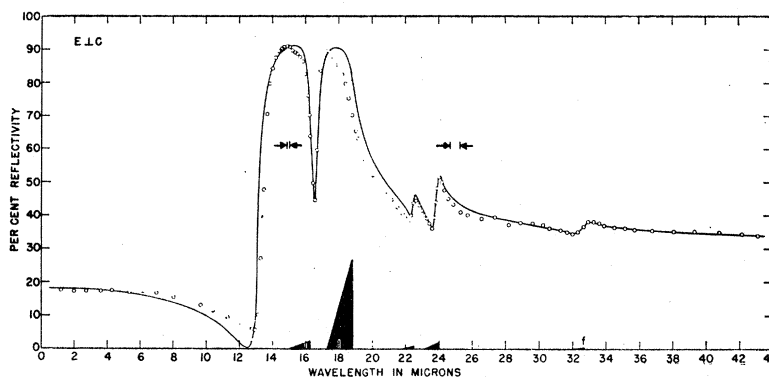
RESULTS

The reflectivity results are shown in Figs. 1 and 2 where the small circles represent the experimental data points and the solid lines represent the best theoretical fit as judged by eye.

For the dispersion analysis, the equations in the introduction were used to compute the reflectivity at 330 wavelength points between 1 and $5000\ \mu$ with most of the points being below $50\ \mu$. No correction was made for the finite angle of incidence (6°) since the correction involved would be smaller than experimental errors.

A method of trial and error was used in fitting theory to experiment, following the suggestions of Spitzer *et al.*⁸ The input data consisted of the oscillator dispersion parameters plus the value of ϵ_∞ . Initial inspection of the experimental data usually correctly dictated the number of oscillators needed and their approximate frequencies. The values which the reflectivity ap-

FIG. 2. Reflectivity of Cr_2O_3 for $E\perp C$ (5-mode fit).



⁷ A. Mitsuishi, Y. Yamada, and S. Fujita, *J. Phys. Chem. Solids* **11**, 131 (1959).

⁸ W. G. Spitzer, K. Kleinman, and D. Walsh, *Phys. Rev.* **113**, 126 (1962).

TABLE I. Classical oscillator parameters Cr₂O₃.

Mode designation	ν_j (cm ⁻¹) (= ν_{TO})	λ_j (μ)	$4\pi\rho_j$	γ_j (cm ⁻¹)	ν_{LO} (cm ⁻¹)
<i>E</i> <i>C</i> (2-mode fit) ^a					
<i>p</i>	538 ± 1%	18.6	5.1 ± 5%	18.0 ± 10%	602 ± 2%
<i>p</i>	613 ± 1%	16.3	0.50 ± 15%	9.0 ± 15%	759 ± 1%
<i>E</i> <i>C</i> (5-mode fit)					
<i>f</i>	303	33.0	0.10	10.0	
<i>f</i>	419	23.9	0.05	5.0	
<i>f</i>	444	22.5	0.12	6.0	
<i>p</i>	538	18.6	4.9	18.0	
<i>p</i>	613	16.3	0.43	9.0	
<i>E</i> ⊥ <i>C</i> (4-mode fit) ^b					
<i>p</i>	417 ± 1%	24.0	0.40 ± 15%	8.0 ± 15%	420 ± 2%
<i>p</i>	444 ± 1%	22.5	0.15 ± 20%	7.0 ± 15%	446 ± 2%
<i>p</i>	532 ± 1%	18.8	5.45 ± 5%	15.0 ± 10%	602 ± 2%
<i>p</i>	613 ± 1%	16.3	0.50 ± 15%	12.0 ± 10%	766 ± 2%
<i>E</i> ⊥ <i>C</i> (5-mode fit)					
<i>f</i>	306	32.7	0.10	10.0	
<i>p</i>	417	24.0	0.40	8.0	
<i>p</i>	444	22.5	0.15	7.0	
<i>p</i>	532	18.8	5.35	15.0	
<i>p</i>	613	16.3	0.50	12.0	

^a All *E*||*C* cases have $\epsilon_\infty = 6.10$ and $\epsilon_0 = 11.7$.

^b All *E*⊥*C* cases have $\epsilon_\infty = 6.20$ and $\epsilon_0 = 12.7$.

proached at short and long wavelengths were useful in giving estimates for ϵ_∞ and ϵ_0 , respectively.

From here the problem became one of appropriately distributing the ρ_j 's and assigning γ_j 's to each of the chosen oscillators. Since the manner in which adjustment of these parameters affects the reflectivity curve is complex, many trials were required to obtain a reasonably good fit.

The final results including uncertainties are tabulated in Table I. The mode designations *p* or *f* stand for permitted or forbidden modes, the permitted modes having strengths equal to or greater than 0.15. The ν_j 's were determined to within 1%. The uncertainties have been assigned by noting that deviation of the parameters by the indicated amount resulted in a significantly poorer fit.

The data could be fitted well in the region of the main reflectivity peaks by two modes for *E*||*C* and 4-modes for *E*⊥*C*. This is consonant with the number of modes permitted by the symmetry of the lattice vibrations of Cr₂O₃.^{2,3} However, the data indicate that the addition of extra weaker modes would improve the fit on the long-wavelength side of the main peaks.⁹ When these modes were added, their strengths were borrowed from the stronger modes thereby leaving ϵ_0 unchanged. This technique was used since the over-all shape and magnitude of the reflectivity curve was essentially unchanged except for the immediate wavelength vicinity of the added mode. It was found that just adding the extra modes not only changed ϵ_0 but also changed the peak reflectivity near the stronger modes.

In his study of Al₂O₃, Barker² also found some extra

⁹ The weak (forbidden-mode) peak at 24 μ in the *E*||*C* spectrum (Fig. 1) appears to be genuine and is not the result of the appearance of the stronger (allowed mode) peak in the *E*⊥*C* spectrum (Fig. 2) due to incomplete polarization. With our beam and polarizer we estimate that the *E*⊥*C* peak ($R=0.52$) would appear in the *E*||*C* spectrum as a peak of height $R=0.406$ on a background of $R=0.40$. The observed height is 0.43.

forbidden modes. He noted that these extra modes disappeared after etching the crystal surface and then reappeared after grinding with diamond dust and concluded that the modes originated from surface strains. The single crystal of Cr₂O₃ used in this experiment was polished with diamond paste but not etched so it is assumed that the extra modes observed here are also due to surface strains. The orientation of the *c* axis in our crystal is the one that produces the strongest forbidden modes with *E*⊥*C* in Al₂O₃.

From Maxwell's equations it can be shown that the dielectric constant is zero for longitudinal waves. Hence the long-wavelength longitudinal mode frequencies ν_{LO} were determined from the zeros of ϵ_1 calculated from the classical parameters. From (5), the zeros of ϵ_1 occur where $n^2 = k^2$. The damping or width of all modes was set to zero so this meant that the ν_{LO} 's were located at the points where both *n* and *k* became zero. This method introduces an error in a value of ν_{LO} no greater than about half the value of the damping constant γ for the corresponding transverse mode. The errors listed in Table I include this.

The errors in measuring the reflectivity of our sample (less than 2% of *R*) are small compared to the error a poor surface can introduce, especially in the maximum values of *R*. As Barker² has shown the polishing procedure not only can lower the maxima in *R*, but can increase the strengths of the forbidden modes. Such effects will not strongly alter the transverse optic (TO) frequencies but could alter the strengths and widths of the modes, and through the strengths, the longitudinal optic (LO) frequencies. However, the consistency of our data with Eq. (7) is some indication of the correctness of the ν_{LO} values, although not assurance that each value of ν_{LO} is free of the effects of our surface. The errors assigned to the dispersion parameters in Table I do not include an estimate of errors due to surface condition.

The absorption of infrared light by ionic crystals is strongly peaked at ν_{TO} . Absorption measurements by others¹⁰ on variously prepared powders of Cr₂O₃ have detected three or four infrared absorption bands at frequencies close to some of the ν_{TO} 's of the allowed modes listed in Table I, but there is certainly no one-to-one correspondence due to difficulties in making measurements on powders.

Table II shows how well the values of the static dielectric constant for the two polarization directions

TABLE II. Comparative values of ϵ_0 of Cr₂O₃.

Orientation	Present work	2 Mc/sec ^a	1 kc/sec ^a
<i>E</i> <i>C</i>	11.7 ± 0.3	11.8	11.9
<i>E</i> ⊥ <i>C</i>	12.7 ± 0.3	13.0	13.3

^a See Ref. 11.

¹⁰ C. Wadier, C. Duval, and J. Lecomte, *Compt. Rend.* **257**, 3766 (1963).

determined in this work compare with those obtained by Fang and Brower.¹¹ The values quoted are the average values they determined from capacitance measurements of a single crystal of Cr₂O₃.

DISCUSSION

For cubic crystals with two atoms per unit cell, it has been shown¹² that

$$(\nu_{LO}/\nu_{TO})^2 = \epsilon_0/\epsilon_\infty. \quad (6)$$

Kurosawa,¹³ and Cochran and Cowley¹⁴ have derived a generalized form of (6) valid for a crystal of any symmetry which can be written as

$$\prod_j \left(\frac{\nu_j(LO)}{\nu_j(TO)} \right)^2 = \frac{\epsilon_0}{\epsilon_\infty}. \quad (7)$$

Application of (7) to the frequencies listed in Table I produced the gratifying results given in Table III. This analysis admittedly does not serve as an individual check on the frequencies of each mode but offers experimental verification of (7).

Table IV lists the parameters for Al₂O₃ given by Barker² and the parameters for Cr₂O₃ determined in this work. It shows that the dielectric constants for both polarization directions are larger by varying degrees for Cr₂O₃ than for Al₂O₃. Fang and Brower¹² have noted from their results, and it is apparent here also, that the orientation which has the larger static dielectric constant is opposite in the two materials.

From Table IV one notes that the frequency of the strongest $E\parallel C$ mode in Al₂O₃ is lower than that in Cr₂O₃, while for $E\perp C$ the frequencies of the two strong-

TABLE III. Comparison of right and left sides of (7) for Cr₂O₃.

Orientation	$\epsilon_0/\epsilon_\infty$	$\prod_j \left(\frac{\nu_j(LO)}{\nu_j(TO)} \right)^2$
$E\parallel C$	1.918	1.920
$E\perp C$	2.048	2.046

¹¹ P. H. Fang and W. S. Brower, Phys. Rev. **129**, 1561 (1963).

¹² R. H. Lyddane, R. G. Sachs, and E. Teller, Phys. Rev. **59**, 673 (1941).

¹³ T. Kurosawa, J. Phys. Soc. Japan **16**, 1298 (1961).

¹⁴ W. Cochran and R. A. Cowley, J. Phys. Chem. Solids **23**, 447 (1962).

TABLE IV. Comparison of the oscillator parameters of Al₂O₃ and Cr₂O₃.

ν_j (TO) (cm ⁻¹)	Al ₂ O ₃			Cr ₂ O ₃			
	$4\pi\rho_j$	ϵ_∞	ϵ_0	ν_j (TO) (cm ⁻¹)	$4\pi\rho_j$	ϵ_∞	ϵ_0
				($E\parallel C$)			
400	6.8	3.1	11.64	538	5.1	6.10	11.7
583	1.7			613	0.50		
				($E\perp C$)			
385	0.30	3.2	9.5	417	0.40	6.20	12.7
442	2.7			444	0.15		
569	3.0			532	5.45		
635	0.30			613	0.50		

est modes in Al₂O₃ are slightly higher than those in Cr₂O₃, although there are considerable differences in the strengths of these two modes in the two crystals. Since the frequencies will be equal to the square root of an effective force constant divided by an effective ionic mass, a reasonable decrease in the Cr₂O₃ frequencies, compared to those in Al₂O₃, is expected if the bonding is the same. The decrease should come about both because the effective ionic mass is somewhat larger in Cr₂O₃ and because the interionic distances are larger in Cr₂O₃, except for the smallest cation-cation distance along the c axis. The increase in interionic distance reduces the force constants between pairs of ions both for ionic bonding and covalent bonding.^{15,16}

Al₂O₃ is considered to be an ionic crystal,^{15,17} although electronegativity considerations¹⁵ allow for about 20% covalent bonding¹⁸ in Al₂O₃, and slightly more covalency in Cr₂O₃. The clearly larger effective force constant in Cr₂O₃ for $E\parallel C$ and possibly larger force constants for $E\perp C$ indicate that bonding changes from primarily ionic in Al₂O₃ to a type providing larger force constants despite longer bond lengths, i.e., to a larger fraction of covalency. It is not clear how much covalency is needed to provide such an effect. Evidence for Cr-Cr bonds in Cr₂O₃ has been described by Schäffer¹⁹ but the strong $E\parallel C$ mode should consist largely of a motion of the chromium sublattice against the oxygen sublattice, in which Cr-Cr bonds would play only a minor role.

¹⁵ L. Pauling, *Nature of the Chemical Bond* (Cornell University Press, Ithaca, New York 1948), 2nd ed.

¹⁶ W. Gordy, J. Chem. Phys. **14**, 305 (1946).

¹⁷ R. Bersohn, J. Chem. Phys. **29**, 326 (1958).

¹⁸ N. Laurance, E. L. McIrvine, and J. Lambe, J. Phys. Chem. Solids **23**, 515 (1962).

¹⁹ C. E. Schäffer, J. Inorg. Nucl. Chem. **8**, 149 (1958).